

Formulation, Characterization and Ex Vivo skin Permeation of Caffeine Loaded Spanlastic Nanovesicles

Omneya M. Ghozzy*, Galal M. Abdelghani, Hassan M. Elsabbagh

Department of Pharmaceutics, Faculty of Pharmacy, Mansoura University, 35516, Mansoura, Egypt.

Corresponding author: Omneya M. Ghozzy

Received 26 February 2020; Accepted 09 March 2020

Abstract: This study aimed to prepare caffeine (CAF) loaded spanlastic nanovesicles for topical use in order to achieve deep skin penetration and to enhance CAF skin retention by developing a sustained release formulation. Vesicles were prepared with various ratios of span 60: different edge activators (EAs) including (Tween 60, Tween 80 and Tween 20) using thin film hydration technique. The prepared formulations were evaluated for entrapment efficiency% (EE %), particle size (PS) and polydispersity index (PDI) in order to determine the optimum formulation. The optimized formulation F4 (composed of Span 60 and Tween 80 as edge activator at weight ratio of 9:1, respectively) exhibited high EE% (60.77±2.45%), PS of (372.63±3.58 nm) which is suitable for topical drug delivery and its PDI value (0.529±0.10) indicated uniform particle size distribution. Fourier Transform Infrared Spectroscopy, Differential Scanning Calorimetry and X-ray Powder Diffraction indicated the lack of drug-excipients interaction and the presence of CAF in amorphous state. The in vitro drug release and ex vivo permeation study showed more prolonged release of CAF from the optimized CAF-loaded spanlastic formulation than the corresponding control CAF solution. The retained CAF amount in the skin after the application of spanlastic formulation was higher than the control CAF solution. Confocal laser scanning microscopy (CLSM) approved the ability of the optimized nanovesicles to penetrate effectively towards deep skin layers and hair follicles. Statistical analysis of stability study results revealed the physical stability of the optimized formulation over a period of 3 months.

Keywords: Caffeine, Edge activator, Nanovesicles, Skin retention, Spanlastics.

I. INTRODUCTION

Topical route is a preferred drug administration route, mainly for causes of better patient compliance and its few systemic side effects^[1, 2]. However, conventional topical drug delivery systems showed some drawbacks like poor skin retention and low bioavailability^[3].

The colloidal systems for drug delivery, including nanoparticles, liposomes, niosomes, and nanoemulsions have been paid much attention as a tool that improves drug bioavailability both topically and systemically^[4].

Spanlastic vesicles are surfactant-based elastic vesicles, they are prepared from Span which is a nonionic lipophilic surfactant together with edge activators which are bilayer softeners that provide flexibility to this type of vesicles; they could be topically used to improve drug penetration and retention in the skin. They can prolong the drug release over time with a controlled manner. This type of elastic nanovesicles are superior to conventional niosomes due to its elasticity that gives it a great ability to deliver the entrapped materials to deep skin layers by squeezing through the skin pores and channels^[5].

Caffeine (1, 3, 7-trimethylxanthine; CAF) is an alkaloid, which is found in tea leaves, coffee, and cocoa beans^[6]. It was reported that the topical use of caffeine has numerous benefits to the skin; Caffeine with Hydrocortisone was effective in atopic dermatitis treatment^[7], also it can stimulate hair growth through the inhibition of the activity of 5 α -reductase enzyme^[8]. It was effective in the treatment of hyper proliferative skin diseases^[9]. Topical application of CAF inhibited UVB-induced nonmalignant and malignant skin tumors in mice^[10]. Moreover, CAF had an anti-cellulite effect; it improved the 'orange peel' appearance and enhanced the cutaneous microcirculation^[11].

The aim of this study was to prepare CAF-loaded spanlastic vesicles for topical use in order to achieve deep skin penetration and to enhance CAF skin retention by developing a sustained release formulation.

II. MATERIALS AND METHODS

2.1. Materials

Caffeine and Rhodamine B were purchased from Alpha Aesar, Germany. Sorbitan monostearate (span60) and Polyoxyethylene sorbitan monolaurate (Tween 20) were purchased from Loba Chemie, India.

Polyoxyethylene sorbitan monooleate (Tween 80) was purchased from Piochem, Egypt. Polyoxyethylene sorbitan monostearate (Tween 60) was purchased from Sisco Research Laboratories, India. Disodium hydrogen phosphate and potassium dihydrogen orthophosphate and were purchased from Adwic, El-Nasr Pharmaceutical Chemicals Co., Egypt. Acetonitrile HPLC grade and Chloroform were purchased from Fisher Scientific, UK. Deionized water was used throughout this study.

2.2. Methods

Preparation of CAF-Loaded Spanlastics

Several Edge activators including (Tween 60, Tween 80 and Tween 20) were used with span 60 (250 mg total weight) to prepare CAF-loaded spanlastics at Span 60: EA weight ratios of 9:1, 8:2 and 7:3, respectively, by using thin film hydration technique^[12]. Data are shown in Table 1.

Accurately weighed Span 60 and EA were dissolved in 10 mL of chloroform in a well closed bottle by sonication using bath type sonicator (Sonix IV, SS101H230, USA) for 10 minutes to obtain a clear solution which is then transferred into a round bottom flask. Then, chloroform was evaporated at 50°C under vacuum, using rotary evaporator (Wheaton, Chicago, Illinois, USA) at 100 rpm to form a thin film on the walls of the flask, traces of chloroform were removed by letting the flask containing the deposited thin film in a desiccator overnight. CAF (120 mg) was dissolved in 7.5 mL of deionized water and used to hydrate the thin film by rotating the flask in a water bath at 65°C under normal pressure. Then, the vesicle suspension was bath sonicated for 2 minutes and stored at refrigerator (4±1°C) for further studies.

Table 1- Composition of Different Spanlastic Formulations.

Formulation Code	Span 60:EA (weight ratio)	Span60 (mg)	Tween60 (mg)	Tween80 (mg)	Tween20 (mg)	CAF (mg)	Deionized water (mL)
F1	9:1	225	25	-	-	120	7.5
F2	8:2	200	50	-	-	120	7.5
F3	7:3	175	75	-	-	120	7.5
F4	9:1	225	-	25	-	120	7.5
F5	8:2	200	-	50	-	120	7.5
F6	7:3	175	-	75	-	120	7.5
F7	9:1	225	-	-	25	120	7.5
F8	8:2	200	-	-	50	120	7.5
F9	7:3	175	-	-	75	120	7.5

2.3. Characterization of CAF-Loaded Spanlastic Formulations

2.3.1 Entrapment Efficiency % (EE %)

The prepared vesicular dispersions were centrifuged at 13,000 rpm and 4°C by using cooling centrifuge (Acculab CE16-4X100RD, USA) in order to separate the un-entrapped CAF from CAF-loaded spanlastic vesicles, then the amount of CAF in the supernatant was suitably diluted and assayed for free CAF at 273 nm using UV-Visible double beam scanning spectrophotometer (Labomed, INC, UVD-2950, USA). The EE % was calculated through the following relationship^[13]:

$$EE (\%) = \frac{(\text{Weight of total drug} - \text{Weight of free drug})}{\text{Weight of total drug}} \times 100 \quad (1)$$

2.3.2. Determination of Vesicle Size, Zeta Potential and Polydispersity Index

One mL of the prepared dispersion was diluted to 100 mL by using deionized water to get a suitable scattering intensity. The average size, potential as well as the polydispersity index of this dispersion was determined by using particle size analyzer (Zetasizer, ZEN 3600, Malvern Instruments limited, UK).

2.3.3. Transmission Electron Microscopy (TEM)

The morphological examination of the optimized formulation was done by using transmission electron microscope (JEOL-TEM, 100 CX, Japan). One mL of freshly prepared spanlastic dispersion was diluted ten folds using deionized water and sonicated for one minute using an ultrasonic bath sonicator (Sonix IV, SS101H230, USA). Then one drop of this diluted dispersion was dropped onto Formvar-coated copper grids (200 mesh, Science Services, Munich, Germany) and left for one minute so that the vesicles can adhere then the excess sample was absorbed using a filter paper. After complete drying at room temperature, the vesicles were examined at 80 KV.

2.3.4. Fourier Transform Infrared Spectroscopy (FTIR)

Spectroscopic studies of CAF, Span60, Tween 80, lyophilized plain and CAF-loaded optimized formulation were done by using Mattson 5000 FTIR Spectrophotometer (Madison Instruments, Middleton, Wisconsin, USA). The samples were homogeneously mixed with potassium bromide and scanned in the frequency range between 4000 and 400 cm⁻¹.

2.3.5. Differential Scanning Calorimetry (DSC)

The thermal characters were analyzed using differential scanning calorimeter (Perkin-Elmer, New York, USA). Ten mg samples each of CAF, Span 60, their corresponding physical mixture with Tween 80 and lyophilized drug-loaded formulation F4 were placed in standard aluminum pans and scanned over a temperature range of 25–300°C at a heating rate of 10°C/min under nitrogen atmosphere.

2.3.6. X-Ray Powder Diffraction (XRPD)

X-ray diffraction patterns (XRPD) of CAF, Span 60, their corresponding physical mixture with Tween 80 and lyophilized drug-loaded formulation F4 were obtained using Powder X-ray diffractometer (FW 1700 X-ray diffractometer, Philips, Netherlands) which was operated at the voltage and current of 40 kV, 30 mA, respectively. Samples were irradiated with monochromatized Cu K α radiation ($\lambda = 1.542 \text{ \AA}$) and the diffraction pattern was recorded over a 2 θ angular range between 2° and 50° with a step size of 0.05 ° in 2 θ and a 0.5 sec counting per step at room temperature.

2.3.7. In Vitro Drug Release

The in vitro drug release of CAF from spanlastic vesicles and control CAF solution was performed by dialysis method. Dialysis membrane (12000–14000 molecular weight cut off) was soaked in phosphate buffer solution (pH= 5.5) for 24 hours prior the experiment. The membrane was fixed between donor and receptor compartments of diffusion cells providing a diffusion area of 7.07 cm². Samples of spanlastic vesicles and CAF solution (equivalent to 50 mg CAF), were placed in the donor compartment, then the receptor compartment was filled with 100 mL of phosphate buffer solution (pH =5.5). The diffusion cells were kept in a thermostatically controlled shaking incubator (GFL 3033 - Shaking incubator, Germany) that was maintained at 37± 0.5°C and a shaking rate of 100 rpm. At predetermined time intervals of 0.5, 1, 2, 3, 4, 5, 6, 7, 8 and 24 hours, samples of 0.5 mL were taken from the release medium and replaced by an equal volume of the buffer solution. The samples taken were suitably diluted and analyzed spectrophotometrically by using UV–Visible double beam scanning spectrophotometer (Labomed, INC, UVD-2950, USA) at 273 nm.

2.3.8. Release Efficiency % (RE %)

Dissolution efficiency is the area under the release curve within certain time interval (t), expressed as a percentage of the area of the rectangle representing 100% release in the same time (t) [14]. In this study RE % was calculated in the time interval of 0 to 6 hours. The area under the curve was calculated by using GraphPad Prism 5 software (GraphPad Software Inc., San Diego, CA, version 5.03) computer program and RE % was calculated according to the following equation [15].

$$RE\% = \frac{\int_0^t Y \times dt}{Y \times 100 \times t} \times 100 \quad (2)$$

Where Y is the percent of drug released at time t.

2.3.9. Confocal Laser Scanning Microscopy (CLSM)

CLSM was used to evaluate the drug delivery behavior of the optimized formulation F4 within skin layers. The optimized spanlastic formulation F4 was prepared according to the same previously mentioned procedures for the preparation of CAF-loaded spanlastics, with the exception that the deposited thin film was hydrated with 0.02% w/v Rhodamine B aqueous solution instead of CAF solution. Samples of shaved dorsal skin of male albino mice were fixed between donor and receptor compartments of diffusion cells providing a diffusion area of 1.54 cm² and the receptor compartment was filled with 25 mL of

phosphate buffer (pH =7.4), then Rhodamine B-loaded spanlastics and control Rhodamine B aqueous solution were applied on the skin surface and left for 6 hours in a thermostatically controlled shaking incubator (GFL 3033 - Shaking incubator, Germany) at $37 \pm 0.5^\circ\text{C}$ and 100 rpm.

At the end of this experiment, the skin samples were rinsed with deionized water, gently wiped and frozen at -18°C then cut into vertical slices of 10 μm thickness using cryostat (Leica Jung CM1800, Germany), these slices were placed between a glass slide and a cover slip and observed using confocal laser scanning microscope (Leica DM 2500, Germany).

2.3.10. Ex Vivo Skin Permeation

Eight male albino mice (2 groups each of 4 animals) were sacrificed and the dorsal skin was shaved, excised, washed with deionized water and soaked in phosphate buffer solution (pH = 7.4) for 24 hours at refrigeration temperature ($4 \pm 1^\circ\text{C}$) prior the experiment. The skin samples were carefully tied to diffusion cells each of 1.54 cm^2 diffusion area, so that the stratum corneum was facing towards the donor compartment.

The receptor compartment was filled with 10 mL of phosphate buffer (pH =7.4) and samples of spanlastic vesicles F4 and CAF solution were placed in the donor compartment, then the diffusion cells were put into a thermostatically controlled shaking incubator (GFL 3033 - Shaking incubator, Germany) that was adjusted to $37 \pm 0.5^\circ\text{C}$ and a rate of 100 rpm.

At predetermined time intervals of 2, 4, 6 and 8 hours, samples of 500 μL were taken from the release media and replaced by an equal volume of the buffer solution. The withdrawn samples were suitably diluted, filtered through 0.45 μm nylon syringe filter (Olimpeak™, Spain) and the released amounts of the drug were analyzed by using HPLC.

At the end of the ex vivo permeation experiment, the remaining formulations were washed from the skin surface and each skin sample was minced manually with scissors, placed into a beaker containing 50 mL of deionized water and sonicated for 3 hours using bath type sonicator (Sonix IV, SS101H230, USA). The obtained CAF extract was filtered through 0.45 μm nylon syringe filter (Olimpeak™, Spain) and assayed for CAF content using HPLC.

HPLC analysis was performed according to the method provided by Ma et al., 2015^[16] using HPLC system (Knauer, Germany) with Azura P6.1L pump and Azura UV/VIS Detector UVD 2.1L as well as Phenomenex HyperClone 5 μm ODS (C18) 250x4.6 mm column, USA. Mixture of water: acetonitrile (85:15 %v /v, respectively) was used as a mobile phase at a flow rate of 1 mL/min. Samples of 20 μL volume were injected and the retention time was 6.7 min at a wavelength of 273 nm.

The ex vivo permeation data were represented by plotting a graph between cumulative amount CAF permeated ($\mu\text{g}/\text{cm}^2$) and time (hours). The flux (J) ($\mu\text{g}/\text{cm}^2/\text{h}$) was expressed as the slope of the linear part of this curve^[17].

2.3.11. Drug Release Kinetics and Mechanism

The ex vivo release data were fitted into different kinetic models of zero-order (cumulative percentage drug released against time), first-order (log percentage drug remaining against time) and Higuchi model (cumulative percentage drug released against square root of time) in order to determine the release kinetic mechanism coefficients (r^2)^[18].

Models were evaluated by using GraphPad Prism 5 software (GraphPad Software Inc., San Diego, CA, version 5.03) computer program.

2.3.12. Stability Study of the Optimized Formula Suspension

A short-term stability study was performed on the optimized formula F4. The study was carried out on spanlastic suspensions which were placed in air-tight amber-colored glass vials and stored in a refrigerator at $4 \pm 1^\circ\text{C}$ for three months. Samples were taken at predetermined time intervals 1, 2 and 3 months and evaluated for entrapment efficiency % (EE %), % drug remaining, particle size (PS), polydispersity index (PDI) and zeta potential (ZP).

Statistical Analysis

All results were expressed as the mean values \pm SD. The data were analyzed using one-way analysis of variance (ANOVA), and Newman–Keuls test was then used for the pairwise multiple comparisons between groups. Where, unpaired student t-test was used in the ex vivo permeation study. Differences were considered significant at ($p < 0.05$).

III. RESULTS AND DISCUSSION

The effect of different weight ratios of Span 60: EAs on EE %, vesicles size and PDI of CAF-loaded spanlastic vesicles is illustrated in Table 2.

3.1 Entrapment Efficiency %

The entrapment efficiency is one of the most important characteristics in the optimization of nanovesicles. The EE% of the prepared spanlastic formulations ranged between 18.93±2.29 and 63.13±3.35% (Table 2).

Table 2- Entrapment efficiency (EE %), Particle size (PS), Polydispersity index (PDI) and Release efficiency (RE_{0-6 hrs} %) of the prepared CAF-loaded spanlastic vesicles. Values are expressed as mean±S.D (n=3).

Formulation Code	EE%	PS(nm)	PDI	RE_(0-6hrs)%
F1	63.13±3.35	390.67±8.08	0.547±0.02	32.27±0.89
F2	53.03±3.95	358.90±7.97	0.437±0.02	35.35±1.65
F3	40.40±3.76	324.57±9.26	0.381±0.03	40.63±1.44
F4	60.77±2.45	372.63±3.58	0.529±0.10	34.63±1.81
F5	48.07±5.36	339.67±13.24	0.488±0.04	38.78±1.56
F6	31.10±2.07	283.17±3.61	0.412±0.05	49.19±1.83
F7	55.10±2.95	350.80±10.25	0.554±0.04	37.51±1.59
F8	38.77±4.18	314.27±4.76	0.519±0.05	42.26±1.92
F9	18.93±2.29	243.47±3.61	0.470±0.09	56.30±2.23

3.1.1 Effect of Edge Activator Type on Entrapment Efficiency %

Statistical analysis of the obtained results in Table 2 showed a significant decrease ($p < 0.05$) in EE% of vesicles prepared with Tween 20 as an EA than those of Tween 60 and Tween 80. This might be due to the shorter alkyl chain of Tween 20 (12-C atoms) compared to Span 60 (18-C atoms), this short chain may perturb the integrity of the vesicular bilayer leading to drug leakage. This finding is in agreement with Hao et al., 2002^[19] who suggested that increasing the alkyl chain length is leading to higher entrapment efficiency.

In regard to vesicles prepared with Tween 60 and Tween 80 as EA, an insignificant ($p < 0.05$) difference was detected between their EE% at 9:1 weight ratio. This might be due the equal length of the alkyl chains of both surfactants. However, vesicles prepared with Tween 80 showed significantly ($p < 0.05$) lower EE% than those prepared with Tween 60 at 8:2 and 7:3 (span 60: EA, respectively) weight ratios. This might be due to the presence of enough weight ratio of Tween 80 which has an unsaturated alkyl chain. This unsaturation enhanced the chain mobility, lowered the phase transition temperature, increased bilayer fluidity and permeability and thus decreased EE%^[19, 20].

In other words, the surfactant HLB value directly affected the drug EE%^[21]. Vesicles could be arranged according to their EE% in the following order: vesicles prepared with Tween 60 (HLB=14.9) > Tween 80 (HLB=15) > Tween 20 (HLB=16.7). Thus, it was clear that there was an inverse relationship between the HLB value of the surfactant and the EE%, this result is in agreement with that reported by Abdelbary and El-gendy, 2008^[22] and El-Laithy et al., 2011^[23].

3.1.2 Effect of Edge Activator Amount on Entrapment Efficiency %

The obtained results showed a significant decrease ($p < 0.05$) in EE% with increasing the EA amount (Table 2). Edge activators are bilayer softening component that increase lipid bilayer flexibility and permeability^[24]. As well these hydrophilic surfactants could enhance the fluidization of the vesicular bilayer^[1, 25]. Thus, the increase of EA amount led to increase in membrane fluidity causing drug leakage to the surrounding aqueous phase.

3.2 Particle Size

The particle size of the prepared formulations was between 243.47±3.61 and 390.67±8.08 nm (Table 2).

Verma et al., 2003^[26] found that vesicles with a size of 600 nm or more didn't have the ability to deliver the entrapped drug to deep skin layers. These vesicles tend to accumulate in or on the stratum corneum and resulted in the formation of a lipid film on the skin upon drying, enhancing the barrier properties of stratum corneum. In the present study, the particle sizes of the prepared spanlastic formulations were considered to be suitable for topical drug delivery.

3.2.1 Effect of Edge Activator Type on Particle Size

Statistical analysis of the obtained results showed that EA had a significant effect ($p < 0.05$) on the mean size of the prepared vesicles.

According to the effect of EA type on the vesicle size, vesicle size can be arranged in the following order: Tween 60 > Tween 80 > Tween 20. This could be explained by the fact that increasing the HLB value results in gradual decrease in the water-oil interfacial tension, thus enhancing vesicles solubilization and decreasing their size^[27]. It was reported by Abbas and Kamel 2019^[5] and Kamel et al., 2013^[28] that increasing the hydrophilicity of surfactant mixtures produced vesicles of smaller sizes. Also, an inverse relationship between the size of nanoparticles and the surfactant HLB value was reported by Naskar et al., 2006^[27].

Additionally, this finding might be related to the effect of the chemical structure of the EA alkyl chain. Tween 60 (Polyoxyethylene sorbitan monostearate) has a saturated alkyl chain that resulted in the formation of rigid vesicular bilayer. On the contrary, Tween 80 (Polyoxyethylene sorbitan monooleate) has an unsaturated alkyl chain that made the bilayer more flexible and enhanced its bending ability^[19] thus resulted in the formation of smaller vesicles than those of Tween 60. Furthermore, the shortness of Tween 20 (Polyoxyethylene sorbitan monolaurate) alkyl chain than that of Span 60 might resulted in the formation of less packed, less stable vesicular bilayer and consequently smaller vesicles upon sonication.

3.2.2 Effect of Edge Activator Amount on Particle Size

The results in Table 2 showed a significant decrease ($p < 0.05$) in vesicle size with increasing the EA amount; this might be due to the decrease in the interfacial tension upon the use of higher concentrations of the EA. Similar results were obtained in a study on the development of glibenclamide-loaded nanoparticles by Dora et al., 2010^[29].

3.3 Polydispersity Index (PDI)

The ratio of standard deviation to mean vesicle size is defined as PDI value^[15], it provides an indication about the uniformity of the size of vesicles within the prepared suspension. Their values vary from 0 to 1. The higher the PDI value, the lower the uniformity of the vesicle size^[30], PDI value greater than 0.5 is related to a broad size distribution^[31].

In this work, PDI values ranged between 0.381 ± 0.03 and 0.554 ± 0.04 and the PDI value of the optimized formulation was 0.529 ± 0.1 (Table 2), indicating that the sizes of the prepared vesicles are almost homogenous.

3.4 Selection of the Optimum Formulation

The obtained results revealed that 9:1 (Span 60: EA, respectively) weight ratio including F1, F4 and F7 provided the highest drug entrapment efficiency (EE %) for the three types of EAs.

The EE% of F1 ($63.13 \pm 3.35\%$) and F4 ($60.77 \pm 2.45\%$) were significantly ($p < 0.05$) higher than that of F7 ($55.10 \pm 2.95\%$). However, there was no significant difference between the EE% of F1 and F4.

Particle size of F4 (372.63 ± 3.58 nm) was significantly ($p < 0.05$) smaller than that of F1 (390.67 ± 8.08 nm). Therefore, F4 was selected as the optimum formulation and it was subjected to further characterization and evaluation for its zeta potential (ZP), Transmission electron microscopy (TEM), Fourier transform infrared spectroscopy (FTIR), Differential scanning calorimetry (DSC), X-ray powder diffraction (XRPD), Confocal laser scanning microscopy (CLSM), ex vivo skin permeation and stability study.

3.5 Zeta Potential

Zeta potential value of the optimized formulation F4 was -39.10 ± 0.79 mv indicating good physical stability. The higher is an absolute zeta potential value, the more the possibility that the vesicular suspension will be stable^[32]. A higher electric charge on the vesicles surfaces can prevent their aggregation because of the repulsion force between them. It was reported by Honary and Zahir, 2013^[33] according to Wissinga et al., 2004^[34] and Jacobs et al., 2000^[35] that an absolute ZP value in the range of -5 mV to +5 mV indicates fast aggregation, about 20 mV indicates short term stability, above 30 mV indicates good stability and above 60 mV indicates excellent stability.

3.6 Transmission Electron Microscopy (TEM)

Figure 1 shows the nanovesicles of the optimized formulation F4, the vesicles were spherical, with uniform size distribution, with no aggregation and their diameters were in agreement with that detected by zetasizer.

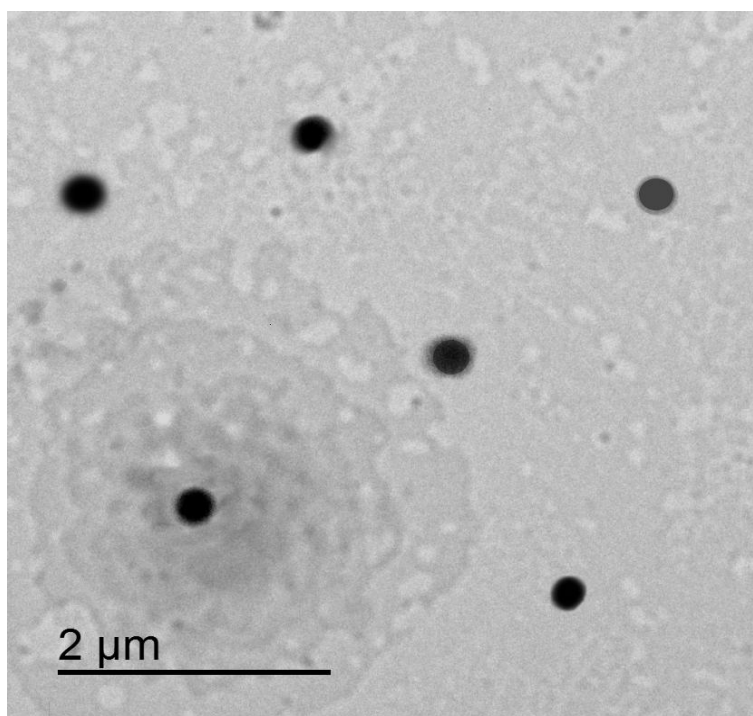


Figure 1-TEM micrograph of F4 spanlastic vesicles.

3.7 Fourier Transform Infrared Spectroscopy (FTIR)

Figure 2 shows the FT-IR spectra of CAF, Span 60, Tween 80, their corresponding physical mixture, lyophilized plain and CAF-loaded optimized formulation (F4).

Two characteristic strong bands at 1702 and 1660 cm^{-1} were observed, these peaks have been attributed mainly to the stretching vibration of carbonyl groups ($> \text{C}=\text{O}$)^[36]. Other bands at 1600 and 1548 cm^{-1} were referred to the $\text{C}=\text{C}$ and $\text{C}=\text{N}$ stretching in the purine ring system^[37]. Aromatic $\text{C}-\text{H}$ stretch appeared at 3112 cm^{-1} and 2954 cm^{-1} . $\text{C}-\text{C}$ stretching within the ring appeared in the frequency range of 1650 to 1400 cm^{-1} . Peaks at 1300 to 1000 cm^{-1} belongs to the couplings of $\text{C}-\text{O}$ and $\text{C}-\text{C}$ stretches of carbonyl groups ($> \text{C}=\text{O}$). The out-of-plane bending of ring $\text{C}-\text{H}$ bonds of aromatic and heteroaromatic compounds gives rise to strong IR bands in the range between 910 and 650 cm^{-1} , amines and amides can contribute absorption in this region^[38]. Peaks in the range of $750-400\text{ cm}^{-1}$ indicate in-plane and out of-plane bending coupled with $\text{C}=\text{O}$ group^[36].

The FT-IR spectrum of F4 spanlastic formulation showed that the drug bands did not disappear or majorly shifted and no new bands were noticed. Thus, it could be concluded that there was no interaction between CAF and other excipients.

3.8 Differential Scanning Calorimetry (DSC)

Figure 3 shows DSC thermograms of CAF, Span 60, their corresponding physical mixture with Tween 80 and lyophilized CAF-loaded formulation F4. Thermograms of CAF and Span 60 exhibited sharp endothermic peaks at 234.29 , 58.12°C , respectively.

In the case of drug-loaded formulation, the phase transition temperature of span 60 was shifted from 58.12 to 51.44°C ; this may be due to the effect of the edge activator which perturbs the packing characteristics leading to fluidization of the vesicular bilayer. DSC thermogram of drug-loaded formulation showed the absence of the endothermic peak of CAF, this might be attributed to the presence of CAF in the amorphous state^[39] indicating its entrapment inside the vesicles.

3.9 X-Ray Powder Diffraction (XRPD)

Figure 4 shows the X-ray powder diffraction pattern of CAF, Span 60, their corresponding physical mixture with Tween 80 and lyophilized CAF-loaded formulation F4.

The diffraction pattern of CAF exhibited a sharp high intensity peak at 2-Theta° of 11.9 and lower intensity peaks at 20.5, 23.7, 24, 26.4 and 27, indicating its presence in a crystalline state. Span 60 showed high intensity peak at 2-Theta ° of 21.5 and low intensity peak at 5.9.

The entrapment of CAF into the spanlastic vesicles reduced its crystallinity to a greater extent. The absence of CAF crystal peaks in the case of CAF-loaded vesicles when compared with its corresponding physical mixture with Span 60 indicates the presence of CAF in amorphous state and its entrapment inside the vesicular system.

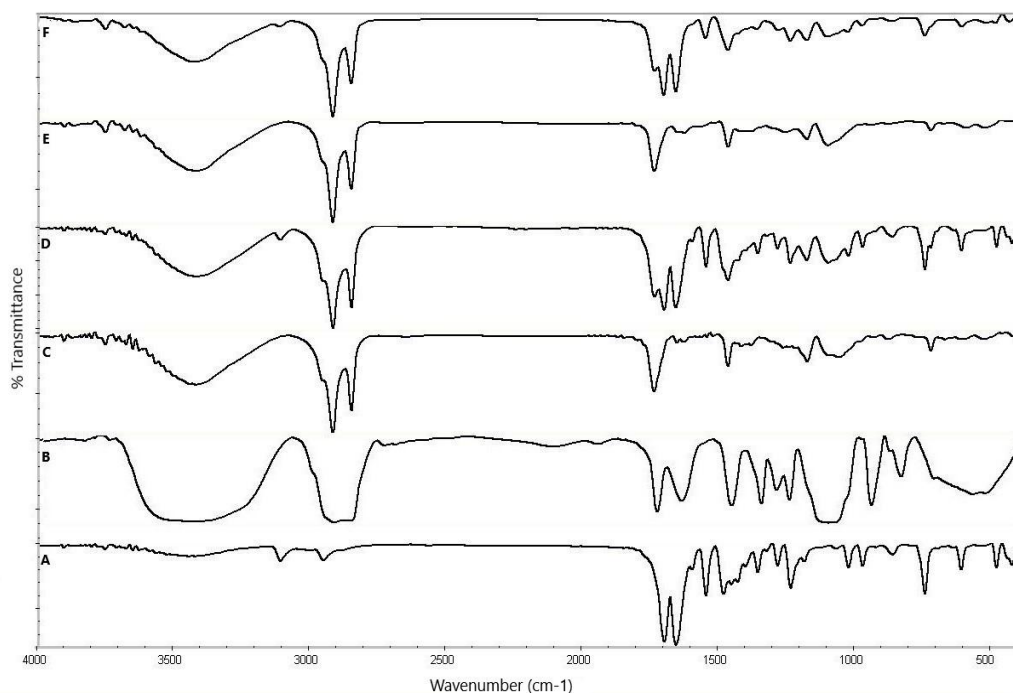


Figure 2- FT-IR spectra of CAF (A), Tween 80 (B), Span 60 (C), Physical mixture of CAF, Span 60 and Tween 80 (D), Plain F4 (E), CAF-loaded F4 (F)

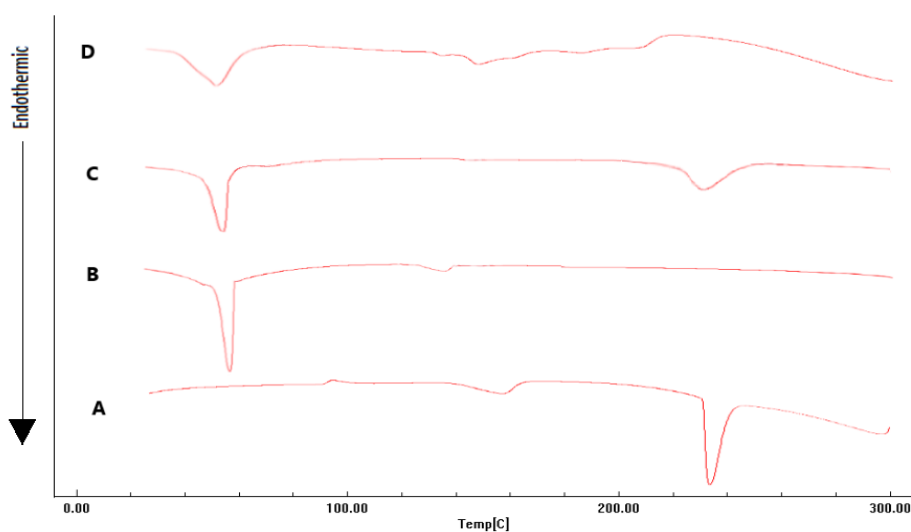


Figure 3- DSC thermograms of CAF (A), Span 60 (B), Physical mixture of CAF, Span 60 and Tween 80 (C), CAF-loaded F4 (D).

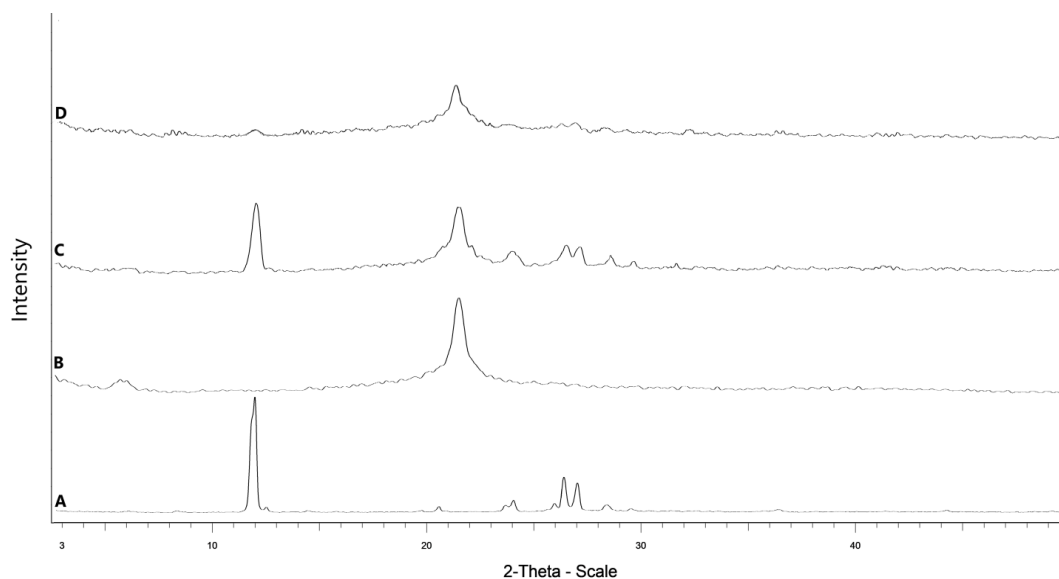


Figure 4- X-ray diffractograms of pure of CAF (A), Span 60 (B), Physical mixture of CAF, Span 60 and Tween 80 (C), CAF-loaded F4 (D).

3.10 In-Vitro Drug Release

The release profiles of CAF from the prepared formulations and its control solution are illustrated in Figures 5-7.

The statistical analysis of $RE_{(0-6)}$ % ranging from 32.27 ± 0.89 to $56.30 \pm 2.23\%$ (Table 2) showed that the release of CAF from all spanlastic formulations was significantly ($P < 0.05$) lower than the corresponding control solution ($81.09 \pm 1.35\%$) indicating sustained release of CAF from all spanlastic formulations. This might be raised to the ability of these vesicles to delay and control the drug release suggesting that they could be a suitable delivery system for the prolonged delivery of CAF.

3.10.1 Effect of EA Type on In-Vitro Drug Release

The in-vitro release results showed that EA type had a significant ($p < 0.05$) effect on $RE_{(0-6)}$ % of the prepared spanlastic vesicles at 8:2 and 7:3 (span 60: EA) weight ratios. Spanlastic formulations prepared using Tween 20 as EA showed a significant ($p < 0.05$) increase in $RE_{(0-6)}$ % compared to vesicles prepared with Tween 60 and Tween 80. Moreover, Tween 80 vesicles showed a significantly higher ($p < 0.05$) release efficiency % than those of Tween 60.

So, According to the effect of the EA type on release efficiency, vesicles could be arranged in the following order: Tween 20 > Tween 80 > Tween 60 and it was concluded that the release efficiency% increased upon increasing the HLB value of the used EA.

3.10.2 Effect of EA Amount on In-Vitro Drug Release

A significant increase ($p < 0.05$) in the release efficiency was found upon increasing the EA amount.

These results could be due to the increase in membrane fluidity and the decrease in vesicle size upon increasing the HLB value of the surfactant mixture forming the vesicular bilayer. These findings are in agreement with Bayindir ZS and Yuksel N, 2010^[40] who reported that increasing the surfactant HLB value decreased vesicular size and increased the release rate.

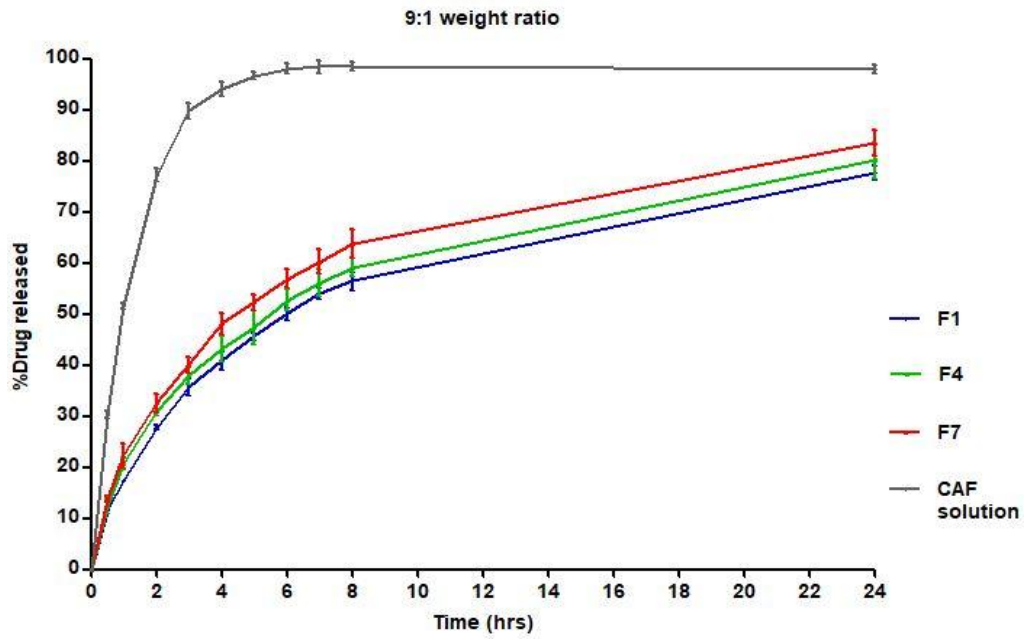


Figure 5- In vitro release profiles of CAF from spanlastic formulations of 9:1 weight ratio and control CAF solution. (n=3)

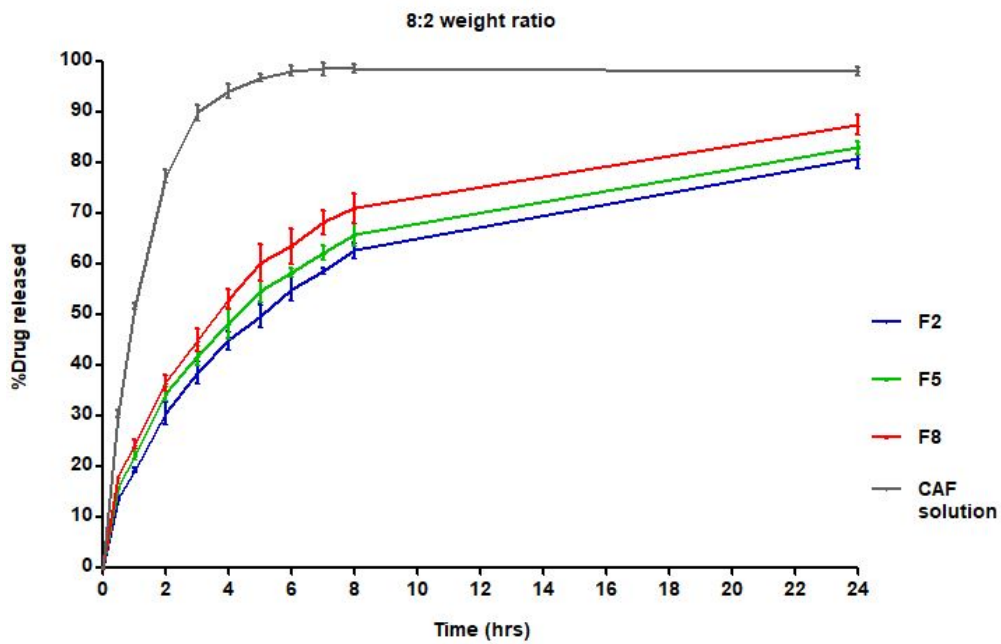


Figure 6- In vitro release profiles of CAF from spanlastic formulations of 8:2 weight ratio and control CAF solution. (n=3)

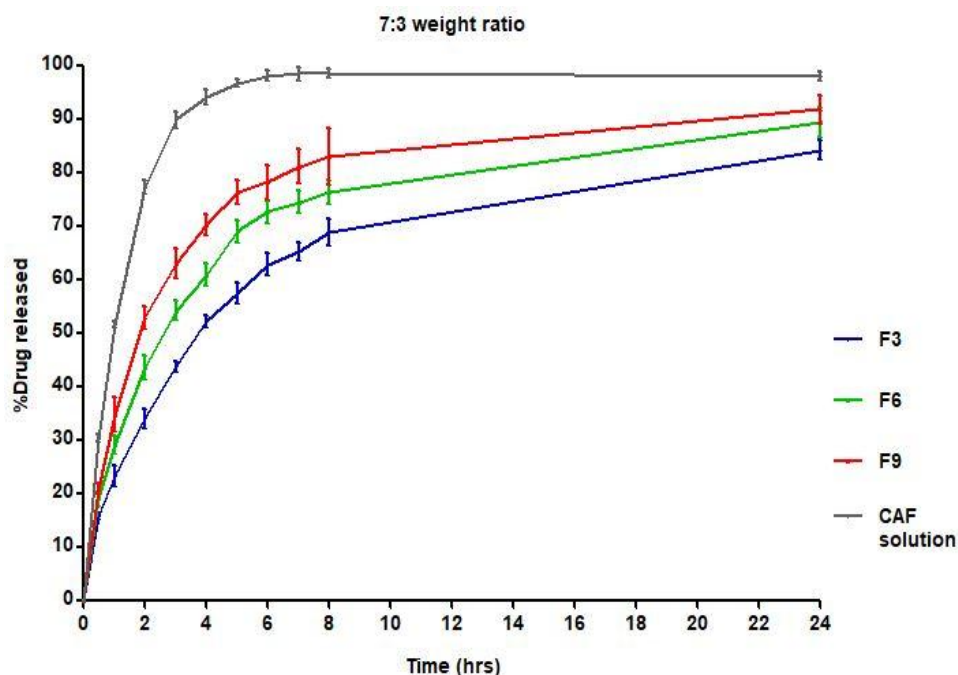


Figure 7- In vitro release profiles of CAF from spanlastic formulations of 7:3 weight ratio and control CAF solution. (n=3)

3.11 Confocal Laser Scanning Microscopy (CLSM)

Figure 8 represents vertical sections of mice skin samples treated with Rhodamine B solution (A) and Rhodamine B-labeled spanlastic formulation F4 (B). Samples treated with Rhodamine B solution showed that the fluorescence was restricted to the superficial skin layer; this may be due to the hydrophilic nature of Rhodamine B. In the case of spanlastic formulation, CLSM approved the ability of these nanovesicles to deliver CAF to deep skin layers including hypodermis. Additionally, the fluorescence was observed in the hair follicles indicating that the follicular pathway might be the dominant way for vesicles penetration into the skin, suggesting that CAF-loaded spanlastic formulation could be a promising tool for follicular targeting of CAF and the stimulation of hair growth.

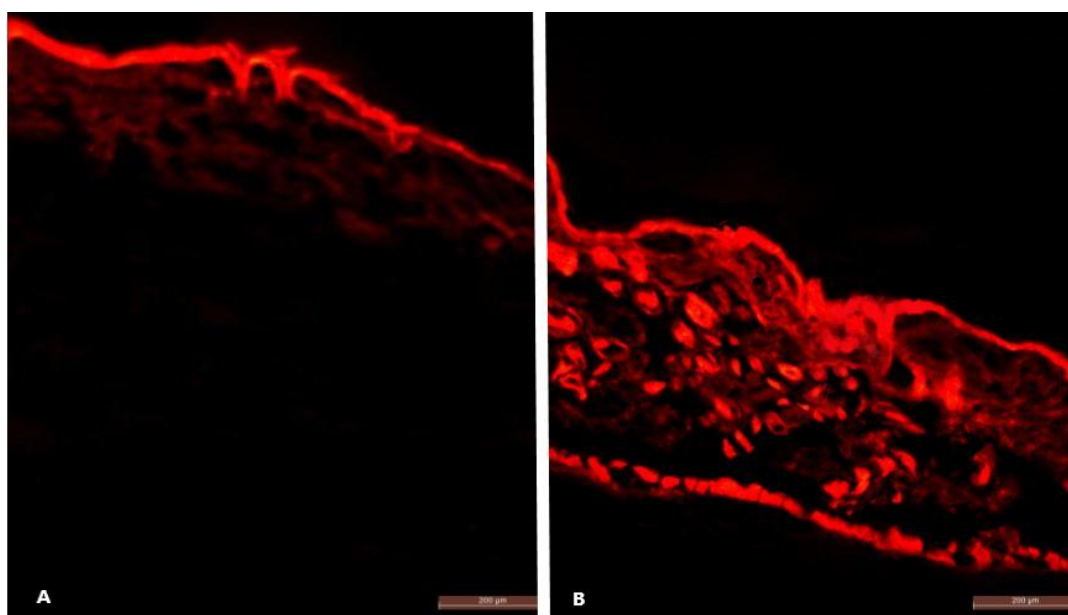


Figure 8- CLSM images of vertical sections of mice skin after application of Rhodamine B solution (A) and Rhodamine B-labeled spanlastic formulation F4 (B)

3.12 Ex Vivo Skin Permeation

The amount of CAF permeated and the amount of CAF retained from the optimized spanlastic formulation F4 and CAF solution through hairless mice skin are shown in Figures 9 and 10, respectively.

The ex vivo skin permeation results revealed that the spanlastic vesicles showed a significantly ($p < 0.05$) lower transdermal flux ($20.26 \pm 0.90 \mu\text{g cm}^{-2} \text{h}^{-1}$) than the corresponding CAF solution ($51.91 \pm 2.61 \mu\text{g cm}^{-2} \text{h}^{-1}$). This result is in agreement with that reported by Touitou et al., 1994^[9] in a study on the ex vivo skin permeation of CAF-loaded liposomes. The amount of CAF permeated through the skin from spanlastic formulation F4 was ($151.53 \pm 18.74 \mu\text{g cm}^{-2}$) which is significantly ($p < 0.05$) lower than that released from the control CAF solution ($372.77 \pm 20.99 \mu\text{g cm}^{-2}$).

The spanlastic system showed a significantly ($p < 0.05$) greater accumulation of CAF in the skin ($234.60 \pm 57.71 \mu\text{g cm}^{-2}$) than the control CAF solution ($73.93 \pm 17.31 \mu\text{g cm}^{-2}$).

These findings indicated that these nanovesicles could act as a drug reservoir in the skin providing prolonged drug release and more drug localization at the site of action. Hence, they could improve the drug therapeutic efficacy.

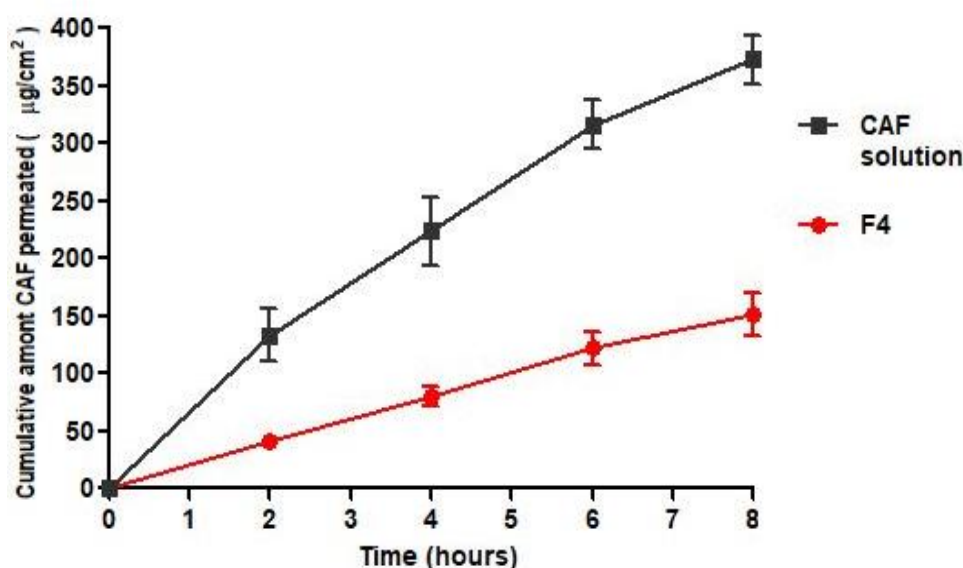


Figure 9- Ex vivo cumulative amount of CAF permeated through mice skin from the optimized CAF-loaded spanlastic formulation F4 and control CAF solution. (n=4)

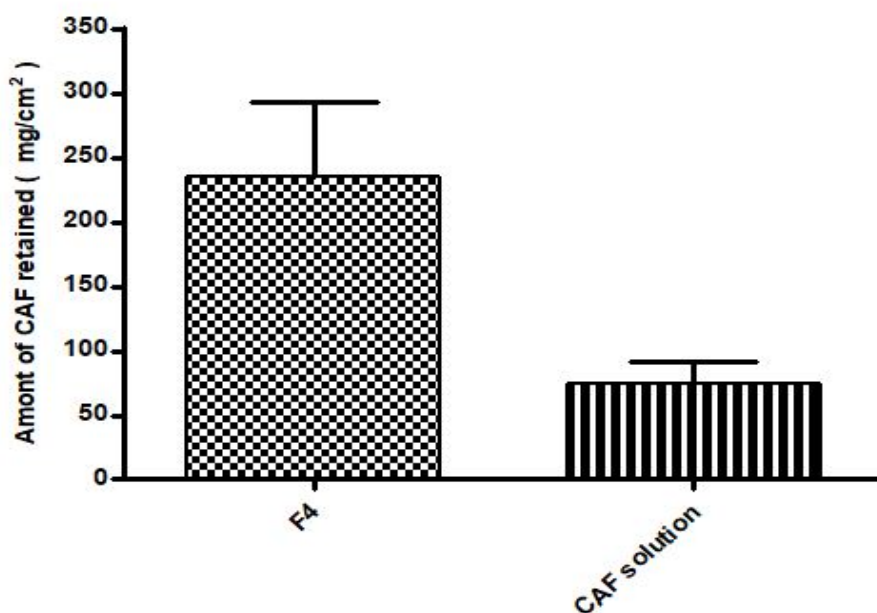


Figure 10- Ex vivo skin retention of CAF from the optimized CAF-loaded spanlastic formulation F4 and control CAF solution after 8 hours of the ex vivo permeation study. (n=4)

3.13 Drug release kinetics and mechanism

Kinetic analysis of the ex vivo release data of the optimized formulation F4 and CAF solution is shown in Table 3. Correlation coefficient (r^2) value of spanlastic vesicles F4 was the highest in zero-order release model indicating consistent release of CAF over time, while that of CAF solution was the highest in first-order kinetic model.

Table 3 - Kinetic analysis for the optimized CAF-loaded spanlastic formulation F4 and CAF solution.

Formulation Code	Correlation coefficient (r^2)			kinetic model
	Zero	First	Higuchi	
F4	<u>0.9651</u>	0.9639	0.9007	Zero order
CAF solution	0.9615	<u>0.9685</u>	0.9533	First order

3.14 Stability Study of the Optimized Formula Suspension

Statistical analysis of stability study results revealed the lack of significant difference ($P > 0.05$) in the EE %, PS, PDI and ZP of the stored formulations compared to freshly prepared one, results are shown in Table 4.

This physical stability might be due to the presence of the vesicular bilayer in solid state at refrigeration temperature preventing drug leakage from vesicles. Moreover, the high zeta potential value prevented the aggregation and fusion of vesicles during storage^[41].

Table 4 - Stability study results of the optimized formula F4. (n=3)

	Initial	1 month	2 months	3 months
EE%	60.77±2.45	59.16±2.30	60.17±1.92	58.97±1.88
% Drug remaining	100%	97.35%	99.01%	97.04%
PS (nm)	372.63±3.58	381.83±7.05	391.13±3.11	397.93±18.75
PDI	0.529±0.10	0.454±0.02	0.487±0.04	0.475±0.03
ZP (mv)	-39.10±0.79	-39.75±0.21	-40.80±1.47	-40.23±0.85

IV. CONCLUSION

In the present study, CAF-loaded spanlastic vesicles were successfully prepared. Confocal laser scanning microscopy approved the ability of these nanovesicles to deliver the encapsulated drug to deep skin layers including hypodermis. The fluorescence was observed also in the hair follicles suggesting that CAF-loaded spanlastic formulation could be a useful tool for follicular targeting of CAF and the stimulation of hair growth. The ex vivo permeation study demonstrated prolonged release of CAF and higher skin retention from spanlastic vesicles than the corresponding CAF solution, providing more drug localization at the site of action. So, it was concluded that these nanovesicles could be a promising tool for topical delivery of CAF.

Conflicts of interest

The authors declare no conflicts of interest.

Ethical approval

Animals were used in this study according to the ethical principles of the scientific committee of Faculty of Pharmacy, Mansoura University, Egypt.

REFERENCES

- [1]. Kakkar, S., & Kaur, I. P., Spanlastics—A novel nanovesicular carrier system for ocular delivery, *International journal of pharmaceutics*, 413(1-2), 2011, 202-210.
- [2]. Tan, X., Feldman, S. R., Chang, J., & Balkrishnan, R., Topical drug delivery systems in dermatology: a review of patient adherence issues, *Expert opinion on drug delivery*, 9(10), 2012, 1263-1271.
- [3]. Singh Malik, D., Mital, N., & Kaur, G., Topical drug delivery systems: a patent review, *Expert opinion on therapeutic patents*, 26(2), 2016, 213-228.
- [4]. Hironaka, K., Inokuchi, Y., Tozuka, Y., Shimazawa, M., Hara, H., & Takeuchi, H., Design and evaluation of a liposomal delivery system targeting the posterior segment of the eye, *Journal of controlled release*, 136(3), 2009, 247-253.

- [5]. Abbas, H., & Kamel, R., Potential role of resveratrol-loaded elastic sorbitan monostearate nanovesicles for the prevention of UV-induced skin damage, *Journal of liposome research*, 2019, 1-9.
- [6]. Ghosh, A. K., Ghosh, C., & Gupta, A., A simple approach to detect caffeine in tea beverages, *Journal of agricultural and food chemistry*, 61(16), 2013, 3814-3820.
- [7]. Fischer, T. W., Hipler, U. C., & Elsner, P., Effect of caffeine and testosterone on the proliferation of human hair follicles in vitro, *International journal of dermatology*, 46(1), 2007, 27-35.
- [8]. Kaplan, R. J., Daman, L., Rosenberg, E. W., & Feigenbaum, S., Topical use of caffeine with hydrocortisone in the treatment of atopic dermatitis, *Archives of dermatology*, 114(1), 1978, 60-62.
- [9]. Touitou, E., Levi-Schaffer, F., Dayan, N., Alhaique, F., & Ricciari, F., Modulation of caffeine skin delivery by carrier design: liposomes versus permeation enhancers, *International journal of pharmaceuticals*, 103(2), 1994, 131-136.
- [10]. Lu, Y. P., Lou, Y. R., Xie, J. G., Peng, Q. Y., Liao, J., Yang, C. S., & Conney, A. H., Topical applications of caffeine or (-)-epigallocatechin gallate (EGCG) inhibit carcinogenesis and selectively increase apoptosis in UVB-induced skin tumors in mice, *Proceedings of the National Academy of Sciences*, 99(19), 2002, 12455-12460.
- [11]. Bertin, C., Zunino, H., Pittet, J. C., Beau, P., Pineau, P., Massonneau, M., ... & Hopkins, J., A double-blind evaluation of the activity of an anti-cellulite product containing retinol, caffeine, and ruscogenine by a combination of several non-invasive methods, *Journal of cosmetic science*, 52(4), 2001, 199-210.
- [12]. Bangham, A. D., Standish, M. M., & Watkins, J. C., Diffusion of univalent ions across the lamellae of swollen phospholipids, *Journal of molecular biology*, 13(1), 1965, 238-IN27.
- [13]. Bansal, S., Aggarwal, G., Chandel, P., & Harikumar, S. L., Design and development of cefdinir niosomes for oral delivery, *Journal of pharmacy & bioallied sciences*, 5(4), 2013, 318.
- [14]. Khan, K. A., The concept of dissolution efficiency, *Journal of pharmacy and pharmacology*, 27(1), 1975, 48-49.
- [15]. ElMeshad, A. N., & Mohsen, A. M., Enhanced corneal permeation and antimycotic activity of itraconazole against *Candida albicans* via a novel nanosystem vesicle, *Drug delivery*, 23(7), 2016, 2115-2123.
- [16]. Ma, H., Yu, M., Lei, M., Tan, F., & Li, N., A novel topical targeting system of caffeine microemulsion for inhibiting UVB-induced skin tumor: characterization, optimization, and evaluation, *AAPS PharmSciTech*, 16(4), 2015, 905-913.
- [17]. Tuntiyasawasdikul, S., Limpongsa, E., Jaipakdee, N., & Sripanidkulchai, B., Effects of vehicles and enhancers on the skin permeation of phytoestrogenic diarylheptanoids from *Curcuma comosa*, *AAPS PharmSciTech*, 18(3), 2017, 895-903.
- [18]. Dash, S., Murthy, P. N., Nath, L., & Chowdhury, P., Kinetic modeling on drug release from controlled drug delivery systems, *Acta Pol Pharm*, 67(3), 2010, 217-23.
- [19]. Hao, Y., Zhao, F., Li, N., & Yang, Y., Studies on a high encapsulation of colchicine by a niosome system, *International journal of pharmaceuticals*, 244(1-2), 2002, 73-80.
- [20]. Ruckmani, K., & Sankar, V., Formulation and optimization of zidovudine niosomes, *AAPS PharmSciTech*, 11(3), 2010, 1119-1127.
- [21]. NVS, M., & Saini, A., Niosomes: a novel drug delivery system, *Int. J. Res. Pharm. Chem*, 1(3), 2011, 498-511.
- [22]. Abdelbary, G., & El-gendy, N., Niosome-encapsulated gentamicin for ophthalmic controlled delivery, *AAPS PharmSciTech*, 9(3), 2008, 740-747.
- [23]. El-Laithy, H. M., Shoukry, O., & Mahran, L. G., Novel sugar esters proniosomes for transdermal delivery of vinpocetine: preclinical and clinical studies, *European journal of pharmaceuticals and biopharmaceuticals*, 77(1), 2011, 43-55.
- [24]. Jacob, L., & Kr, A., A review on surfactants as edge activators in ultradeformable vesicles for enhanced skin delivery, *International Journal of Pharma and Bio Sciences*, 4(3), 2013, 337-44.
- [25]. Trotta, M., Peira, E., Debernardi, F., & Gallarate, M., Elastic liposomes for skin delivery of dipotassium glycyrrhizinate, *International journal of pharmaceuticals*, 241(2), 2002, 319-327.
- [26]. Verma, D. D., Verma, S., Blume, G., & Fahr, A., Particle size of liposomes influences dermal delivery of substances into skin, *International journal of pharmaceuticals*, 258(1-2), 2003, 141-151.
- [27]. Naskar, M. K., Patra, A., & Chatterjee, M., Understanding the role of surfactants on the preparation of ZnS nanocrystals, *Journal of Colloid and Interface science*, 297(1), 2006, 271-275.
- [28]. Kamel, R., Basha, M., & Abd El-Alim, S. H., Development of a novel vesicular system using a binary mixture of sorbitan monostearate and polyethylene glycol fatty acid esters for rectal delivery of rutin, *Journal of liposome research*, 23(1), 2013, 28-36.
- [29]. Dora, C. P., Singh, S. K., Kumar, S., Datusalia, A. K., & Deep, A., Development and characterization of nanoparticles of glibenclamide by solvent displacement method, *Acta Pol Pharm*, 67(3), 2010, 283-90.

- [30]. Shakeel, F., Baboota, S., Ahuja, A., Ali, J., Aqil, M., & Shafiq, S., Nanoemulsions as vehicles for transdermal delivery of aceclofenac. *AAPS PharmSciTech*, 8(4), 2007, 191.
- [31]. Wu, L., Zhang, J., & Watanabe, W., Physical and chemical stability of drug nanoparticles. *Advanced drug delivery reviews*, 63(6), 2011, 456-469.
- [32]. Ostolska, I., & Wiśniewska, M., Application of the zeta potential measurements to explanation of colloidal Cr 2 O 3 stability mechanism in the presence of the ionic polyamino acids. *Colloid and polymer science*, 292(10), 2014, 2453-2464.
- [33]. Honary, S., & Zahir, F., Effect of zeta potential on the properties of nano-drug delivery systems-a review (Part 2). *Tropical Journal of Pharmaceutical Research*, 12(2), 2013, 265-273.
- [34]. Wissing, S. A., Kayser, O., & Müller, R. H., Solid lipid nanoparticles for parenteral drug delivery. *Advanced drug delivery reviews*, 56(9), 2004, 1257-1272.
- [35]. Jacobs, C., Kayser, O., & Müller, R. H., Nanosuspensions as a new approach for the formulation for the poorly soluble drug tarazepide. *International journal of pharmaceutics*, 196(2), 2000, 161-164.
- [36]. Taeye, J. D., & Huyskens, T. Z., Infrared spectrum of caffeine and its hydrochloride dihydrate. *Spectroscopy letters*, 19(4), 1986, 299-310.
- [37]. Nafisi, S., Shamloo, D. S., Mohajerani, N., & Omid, A., A comparative study of caffeine and theophylline binding to Mg (II) and Ca (II) ions: studied by FTIR and UV spectroscopic methods. *Journal of molecular structure*, 608(1), 2002, 1-7.
- [38]. Hsu, C. P. S., Infrared spectroscopy Handbook of Instrumental Techniques for Analytical Chemistry, Frank A. Settle. Prentice Hall PTR: Upper Saddle River, 1997, 995.
- [39]. Elsharif, N. I., Shamma, R. N., & Abdelbary, G., Terbinafine hydrochloride trans-ungual delivery via nanovesicular systems: in vitro characterization and ex vivo evaluation, *AAPS PharmSciTech*, 18(2), 2017, 551-562.
- [40]. Bayindir, Z. S., & Yuksel, N., Characterization of niosomes prepared with various nonionic surfactants for paclitaxel oral delivery, *Journal of pharmaceutical sciences*, 99(4), 2010, 2049-2060.
- [41]. Farghaly, D. A., Aboelwafa, A. A., Hamza, M. Y., & Mohamed, M. I., Topical delivery of fenoprofen calcium via elastic nano-vesicular spanlastics: optimization using experimental design and in vivo evaluation, *AAPS PharmSciTech*, 18(8), 2017, 2898-2909.

Omneya M. Ghoszy, et al. "Formulation, Characterization and Ex Vivo skin Permeation of Caffeine Loaded Spanlastic Nanovesicles." *IOSR Journal of Pharmacy (IOSRPHR)*, 10(2), 2020, pp. 01-15.